

Article

Mathematical Modeling: Cisplatin Binding to Deoxyribonucleic Acid

Mansoor H. Alshehri 

Department of Mathematics, College of Science, King Saud University, P.O. Box 2455, Riyadh 11451, Saudi Arabia; mhalshehri@ksu.edu.sa

Abstract: The discovery of the cisplatin drug attracted considerable research attention as scientists strove to understand the drug's mechanism in the human body that is responsible for destroying cancer cells, particularly the coordination between the cisplatin drug and deoxyribonucleic acid. Here, the binding energies of a cisplatin molecule relative to double-stranded deoxyribonucleic acid are obtained. The interactions of the system are determined by performing double integrals, and the analytical expressions are derived from the Lennard–Jones function and the continuum approximation; here, it is assumed that a discrete atomic structure might be replaced by surfaces with a constant average atomic density. The results observed that the cisplatin molecule is binding to the double-stranded deoxyribonucleic acid at either the minor or major grooves. By minimizing the interaction energies between the cisplatin molecule and the minor and major grooves, for arbitrary distances λ and arbitrary tilt angles φ from the axis of the helix of the double-stranded deoxyribonucleic acid, the binding energies are determined, and their values are ≈ -6 and ≈ -12.5 (kcal/mol), respectively. Thus, we may deduce that the major groove in double-stranded deoxyribonucleic acid is the most preferred groove for linking with the cisplatin molecule. The current analysis might help in the equivalent continuum modeling of deoxyribonucleic acids and nanocomposites.

Keywords: double-stranded DNA; mathematical modeling; cisplatin; continuum approximation; Lennard–Jones potential

MSC: 92-XX; 92-08



Citation: Alshehri, M.H.

Mathematical Modeling: Cisplatin Binding to Deoxyribonucleic Acid. *Mathematics* **2023**, *11*, 235. <https://doi.org/10.3390/math11010235>

Academic Editors: Ricardo Lopez-Ruiz and Mostafa Bendahmane

Received: 19 November 2022

Revised: 13 December 2022

Accepted: 26 December 2022

Published: 3 January 2023



Copyright: © 2023 by the author. Licensee MDPI, Basel, Switzerland. This article is an open access article distributed under the terms and conditions of the Creative Commons Attribution (CC BY) license (<https://creativecommons.org/licenses/by/4.0/>).

1. Introduction

Recently, the characterization of nanostructures and the realization and design of nanomaterial-based advanced functions with miniature devices generated considerable impact within the area of micro-engineering and modern materials science [1]. Due to their unique geometric, mechanical, and electronic properties and their small sizes, nanomaterials are utilized in medical fields for the purposes of diagnoses and imaging and for gene and drug delivery, and they are also utilized in the manufacturing and industrial sectors [2–4]. Deoxyribonucleic acid (DNA) indicates the molecule that carries the genetic details of an organism. The geometric structure of DNA was discovered in 1954 [5], and its discovery marked the start of a novel scientific age that have converted the foundations of medicine and biology; it also gave rise to the development of novel areas, such as genetic engineering and molecular biology. Double-stranded deoxyribonucleic acid (dsDNA) contains two linked strands, which are twisted around each other, and they are connected by hydrogen bonds between a simple unit of DNA, which is known as nucleotide bases [6]. There are four nucleotides in DNA, which might be either cytosine (C), adenine (A), guanine (G), and thymine (T), and every single turn in the dsDNA has approximately twenty-one nucleotides [6]. Furthermore, dsDNA has two helices and two grooves (minor and major) that are created by coiling the helices around each other; the major groove is wide and deep (≈ 22 Å in length), and the minor groove is narrow and shallow (≈ 12 Å in length) [6]. In

the present study, dsDNA is assumed to be in the B-form, which is the common structure observed inside cells [6,7].

On the other hand, cisplatin (Cis) or cis-diamminedichloroplatinum (II) ($\text{Pt}(\text{NH}_3)_2\text{Cl}_2$) is a well-known chemotherapeutic drug, and it is one of the most effective antitumor drugs [8]. Cisplatin was approved by the Food and Drug Administration (FDA) in 1978, and the treatment rate of testicular cancer is greater than 90% [9]. In addition, Cis drugs have been used for the treatment of numerous types of malignancies, including esophageal, head and neck, ovarian, cervical, bladder, and nonsmall cell lung cancers [8,9]. Although Cis is used to treat certain types of human cancers, the Cis drug has some limitations that result from many side effects of the Cis drug [9]. As DNA is the primary target of cisplatin in cells [9], the details of the interaction energies between the cisplatin and dsDNA molecules are studied to characterize the types of binding interactions.

Despite there being a number of experiments that study the interaction and binding of cisplatin to DNA, the use of conventional applied mathematical modeling is not common in this area. Dutta et al. developed atomic force microscopy (AFM) to study cisplatin-induced DNA bends, and they found that Cis induces a bend angle of 36° , which may make the DNA slightly more flexible at the bend [10]. Wing et al. showed that the binding of Cis relative to the B-DNA double helix can freely move into the major groove in the dsDNA using an X-ray crystal structure analysis [11]. Takahara et al. described the X-ray structure of Cis-DNA adducts, and their results showed that the Cis adducts induced global bending toward the major groove in the double-helix DNA [12,13]. Stella et al. used nuclear magnetic resonance (NMR) to determine the structural binding of two cisplatin molecules on a palindromic sequence of B-DNA where the two Cis molecules are placed 180° around the helix axis [14]. Their results observed that each Cis-GG adduct bends the DNA by approximately 40° , and the helix's axis is dislocated by approximately 13 Å.

Glogowska et al. used Raman optical activity (ROA) spectroscopy to study the interactions between cisplatin and DNA, and they demonstrated that there were no interactions or weak interactions between Pt and adenine and pyrimidines; consequently, N7-guanine monoadducts were created during the first step of the cross-linking process [15]. In addition, other studies showed that guanine-(N7) and adenine-N(3) are the most nucleophilic atoms found in DNA, and the preferred positions for platinum when linking to DNA involve these atoms [15]. Sip et al. employed gel electrophoresis studies and molecular mechanics to obtain structural details about the different site-specific Cis-DNA adducts, and their results observed that the inter-strand adduct bends the double helix at the major groove; the double helix conserves its average twist angle [16]. Gelasco and Lippard showed cisplatin-DNA adduct formations with a kink of around 60° toward the major groove at the platinum coordination site using NMR spectroscopy and simulations with molecular dynamics (MD) [17]. Furthermore, the interactions of Cis-DNA have been investigated using numerous techniques, and most of these studies suggested that Cis targets the major groove in DNA [9,18,19]. Crisafuli et al. characterized the interaction of cisplatin-DNA by performing single-molecule stretching experiments with optical tweezers; they showed that the binding of cisplatin-DNA might be extracted from pure mechanical measurements [20]. Another NMR study indicated that the solution structure of cisplatin-DNA is unwound and bent toward the minor groove [21].

Mechanical formulas, together with classical applied mathematics, may be utilized to model the ideal formula behavior of problems to obtain perfect solutions for them [22–26], where, in the present work, we provide analytical information for the interactions between the dsDNA molecule and the Cis molecule. Furthermore, novel mathematical models are required to secure the full import of nanotechnology into oncology, as Ferrari stated [27]. In this paper, we use the 6–12 Lennard–Jones (L–J) potential function and adopt the continuum approximation applied in [22,24] by assuming that the atoms of the Cis and DNA molecules may be uniformly distributed across their surfaces; thus, the total interaction energies for different non-bonded molecules might be obtained analytically by employing the integration of surfaces. In the following section, the analytical calculations of the

interactions between the Cis and DNA molecules for the special and general cases of the helical phase angle, ψ , are presented. The main target of this study is to understand the binding of cisplatin to dsDNA (as shown in Figure 1, the optimization geometries for the binding of the Cis molecule to DNA), which might provide explanations and information for researchers and assist in finding methods to reduce cellular death during the binding of cisplatin to DNA and the mechanisms of DNA repair. This method may allow an analytical characterization of the interactions between massive molecular structures, such as DNA molecules, and the method can assist other computational approaches in obtaining quicker results.

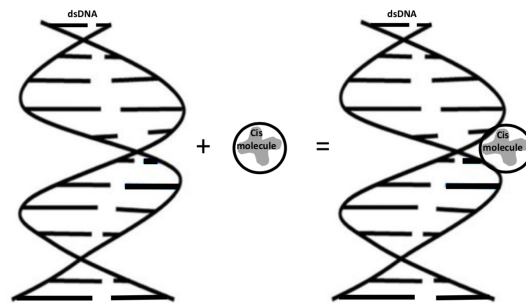


Figure 1. Geometry of a cisplatin molecule binding to dsDNA.

2. Mathematical Modeling

In this section, the analytical expressions for the interactions between the dsDNA and Cis molecules are obtained, and they can be found by employing computer algebra packages, such as Maple. The (6–12) L–J function for unbonded molecules with the continuum approximation is applied to calculate the interactions of the system, which might be obtained by employing the two surface integrals and are provided by the following:

$$E_{tot} = \ell_1 \ell_2 \int_{S_1} \int_{S_2} \left(-\frac{A}{\tau^6} + \frac{B}{\tau^{12}} \right) dS_1 dS_2,$$

where ℓ_1 and ℓ_2 are the atomic surface densities of the two molecules, and τ is the distance between the surfaces of the two molecules. In addition, A and B donate the L–J parameters, and they can be obtained by using the Lorentz–Berthelot mixing rule [28]: where $A = 4\epsilon\sigma^6$ and $B = 4\epsilon\sigma^{12}$, and the values of the van der Waals diameter, σ , and well depth, ϵ , for each atom in the system were taken from [29]. The dsDNA molecule is modeled on a surface with a double helical structure, as shown in Figure 2, and it is assumed to include 10.5 base pairs in the double helix of DNA for a 360° rotation in the B-form. Thus, the coordinates of a point on the surface of the dsDNA is given as

$$\left(\frac{a}{2} \left[\cos \omega + \cos(\omega - \psi) + \varpi \left(\cos \omega - \cos(\omega - \psi) \right) \right], \right. \\ \left. \frac{a}{2} \left[\sin \omega + \sin(\omega - \psi) + \varpi \left(\sin \omega - \sin(\omega - \psi) \right) \right], \frac{q\omega}{2\pi} \right),$$

where ψ is the helical phase angle, $q = 34 \text{ \AA}$ is the unit cell length, $a = 10 \text{ \AA}$ is the radius of the dsDNA helix, and the parametric variables ω and ϖ are such that $-\pi < \omega < \pi$ and $-1 < \varpi < 1$. We comment that the helical curve is parameterized normally by a single parameter, ω , in the present analysis to integrate overall values of the dsDNA radius from 0 to a ; two parameters have been adopted to permit the variable’s internal points of the helicoid.

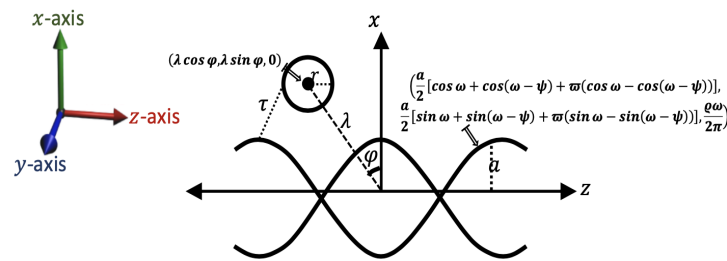


Figure 2. Geometric parameterization of a cisplatin molecule that is binding to dsDNA.

In addition, the Cis molecule is assumed to be at a distance λ from the z -axis of the dsDNA; thus, the coordinates of the center of the Cis molecule are given as $(x, y, 0)$, which may be expressed in terms of the distance λ in the radial direction and a polar angle φ ; that is, $x = \lambda \cos \varphi$ and $y = \lambda \sin \varphi$. Thus, the distance, τ , between the surface of the two molecules (dsDNA and Cis) is given as

$$\tau^2 = \left(\frac{a}{2} \left[\cos \omega + \cos(\omega - \psi) + \varpi (\cos \omega - \cos(\omega - \psi)) \right] - \lambda \cos \varphi \right)^2 + \left(\frac{a}{2} \left[\sin \omega + \sin(\omega - \psi) + \varpi (\sin \omega - \sin(\omega - \psi)) \right] - \lambda \sin \varphi \right)^2 + \left(\frac{\varrho \omega}{2\pi} \right)^2.$$

The mathematical perspective of this study is that several of the integrals will be identified from integral representations of the different functions, such as hypergeometric functions ([30], Section 7.5), and it is given as

$$F(\nu, \xi; \eta; \iota) = \frac{\Gamma(\eta)}{\Gamma(\xi)\Gamma(\eta - \xi)} \int_0^1 \frac{\varkappa^{\xi-1} (1 - \varkappa)^{\eta-\xi-1}}{(1 - \varkappa \iota)^\nu} d\varkappa, \tag{1}$$

where Γ is the usual gamma function. We comment that, for particular surfaces, such integrals might oftentimes be obtained in terms of well-known analytical functions, but these integrations are highly nontrivial in general. Therefore, such mathematical formulas are evaluated numerically through algebraic packages such as MATLAB and MAPLE. Thus, the total interaction, E_{tot} , for the binding energy of the Cis to the dsDNA may be obtained from

$$E_{tot_i} = \frac{\ell_{D_i} a \varrho \sin(\psi/2)}{2\pi} \int_{-\pi}^{\pi} \int_{-1}^1 E_p \sqrt{1 + \left(\frac{2a\pi \sin(\psi/2)}{c} \omega \right)^2} d\omega d\omega, \tag{2}$$

where ℓ_{D_i} is the atomic surface density of the dsDNA ($i \in \{S$ for the special case of $\psi = \pi$ and G for the general case of $\psi = 12\pi/17\}$), and E_p is the interaction energy between a double helix and a point [31], which is given by

$$E_p = \pi r \ell_{Cis} \left\{ -4rA \left[\frac{1}{(\tau^2 - r^2)^3} + \frac{2r^2}{(\tau^2 - r^2)^4} \right] - \frac{4rB}{5} \left[\frac{5}{(\tau^2 - r^2)^6} + \frac{80r^2}{(\tau^2 - r^2)^7} + \frac{336r^4}{(\tau^2 - r^2)^8} + \frac{512r^6}{(\tau^2 - r^2)^9} + \frac{256r^8}{(\tau^2 - r^2)^{10}} \right] \right\}.$$

In the present study, we will use the atomic surface density of the Cis molecule $\ell_{Cis} = 0.165 \text{ \AA}^{-2}$ and the radius of the Cis molecule $r = 2.3 \text{ \AA}$ together with the L–J parameters: $A = 393.683 \text{ (\AA}^6 \text{ kcal/mol)}$ and $B = 635937.288 \text{ (\AA}^{12} \text{ kcal/mol)}$. Firstly, the corresponding calculations for the interaction between Cis and dsDNA for the special case

of the helical phase angle $\psi = \pi$ are presented. Therefore, the distance, τ , in this case, is provided as follows.

$$\begin{aligned} \tau^2 &= (a\omega)^2 - 2a\omega\lambda \cos(\omega - \varphi) + \lambda^2 + (\rho\omega/2\pi)^2 \\ &= (a\omega - \lambda)^2 + 4a\omega\lambda \sin^2(\omega - \varphi/2) + (\rho\omega/2\pi)^2, \end{aligned}$$

Thus, the interaction, E_{tot_s} , for this case, can be obtained from the following:

$$E_{tot_s} = \frac{\ell_{D_s} a \rho}{2\pi} \int_{-\pi}^{\pi} \int_{-1}^1 E_p \sqrt{1 + \left(\frac{2a\pi}{\rho} \omega\right)^2} d\omega d\omega, \tag{3}$$

where $\ell_{D_s} = 0.84 \text{ \AA}^{-2}$. To evaluate these integrals analytically, we define the new integral T_m as

$$T_m = \int_{-1}^1 \int_{-\pi}^{\pi} \left(1 + \frac{4a^2\pi^2}{\rho^2} \omega^2\right)^{1/2} (\tau^2 - r^2)^{-m} d\omega d\omega,$$

where m is a positive integer ($m \in \{3, 4, 6, 7, 8, 9, 10\}$), and

$$\tau^2 = (a\omega)^2 - 2a\omega\lambda \cos(\omega - \varphi) + \lambda^2 + (\rho\omega/2\pi)^2.$$

Now, T_m is evaluated over ω by introducing integral R_m as

$$R_m = a^{-2m} \int_{-1}^1 [\omega^2 - 2\alpha\omega + \beta]^{-m} (1 + \rho\omega^2)^{1/2} d\omega,$$

where $\alpha = \lambda \cos(\omega - \varphi)/a$, $\beta = [\lambda^2 - a^2 + (\rho\omega/2\pi)^2]/a^2$ and $\rho = (2a\pi/\rho)^2$; thus, we have the following.

$$R_m = a^{-2m} \beta^{-m} \int_{-1}^1 (1 + \rho\omega^2)^{1/2} [1 - 2\alpha\omega/\beta + \omega^2/\beta]^{-m} d\omega.$$

By taking $u = \omega/\beta^{1/2}$, we have

$$R_m = a^{-2m} \beta^{-m+1/2} \int_{-1/\beta^{1/2}}^{1/\beta^{1/2}} (1 + \rho\beta u^2)^{1/2} [1 - 2\alpha u/\beta^{1/2} + u^2]^{-m} du,$$

and then expanding the $[1 - 2\alpha u/\beta^{1/2} + u^2]^{-m}$ terms, thus

$$R_m = a^{-2m} \beta^{-m} \alpha \sum_{h=0}^{\infty} C_h^m(x) \int_{-1/\beta^{1/2}}^{1/\beta^{1/2}} u^h (1 + \rho\beta u^2)^{1/2} du,$$

where $C_h^m(x)$ is the usual Gegenbauer polynomial ([32], Section 3.15.1), and $x = \alpha/\beta^{1/2}$. By letting $y = \beta^{1/2}u$, R_m thus becomes

$$R_m = a^{-2m} \sum_{h=0}^{\infty} \beta^{-m-h/2} C_h^m(x) \int_{-1}^1 y^h (1 + \rho y^2)^{1/2} dy,$$

We note that when h is an odd number, the integral is equal to zero; therefore, h can be replaced with $2h$, thus

$$R_m = 2a^{-2m} \sum_{h=0}^{\infty} \beta^{-m-h} C_h^m(x) \int_0^1 y^{2h} (1 + \rho y^2)^{1/2} dy,$$

Now, by taking $w = y^2$, R_m becomes

$$R_m = 2a^{-2m} \sum_{h=0}^{\infty} \beta^{-m-h} C_h^m(x) \int_0^1 w^{h-1/2} (1 + \rho w)^{1/2} dy,$$

and now we can use the hypergeometric function (1) to evaluate this integral. Thus we have R_m as follows.

$$R_m = 2a^{-2m} \sum_{h=0}^{\infty} \beta^{-m-h} C_{2h}^m(x) F(-1/2, h + 1/2; h + 3/2; -\rho) / (2h + 1),$$

In addition, using the definition of the usual hypergeometric function ([30], Section 7.5), which is given as

$$F(t_1, t_2; t_3; l) = \sum_{c=0}^{\infty} \frac{(t_1)_c (t_2)_c}{c! (t_3)_c} l^c,$$

where $(t_b)_c = t_b(t_b + 1)(t_b + 2) \dots (t_b + c - 1)$ is the Pochhammer symbol and $b \in \{1, 2, 3\}$. Moreover, from the generalized hypergeometric series [32], we have

$$C_{2h}^m(x) = (-1)^h \binom{h+m-1}{h} \sum_{j=0}^{\infty} \frac{(-h)_j (h+m)_j}{(1/2)_{jj!}} x^{2j},$$

where $\binom{i}{j}$ denotes the binomial coefficient.

Furthermore, to evaluate T_m over ω , integral Q_m is defined as

$$Q_m = a^{2(m+h)} \lambda^{2j} (\lambda^2 - r^2)^{-m-h-j} W_m,$$

where

$$\begin{aligned} W_m &= \int_{-\pi}^{\pi} \cos^{2j}(\omega - \varphi) \left[1 + \left(\rho^2 / 4\pi^2 (\lambda^2 - r^2) \right) \omega^2 \right]^{-m-h-j} d\omega \\ &= \int_{-\pi}^{\pi} (\cos \omega \cos \varphi + \sin \omega \sin \varphi)^{2j} \left[1 + \gamma \omega^2 \right]^{-m-h-j} d\omega \\ &= \sum_{q=0}^{2j} \binom{2j}{q} \cos^{2j-q} \varphi \sin^q \varphi \int_{-\pi}^{\pi} \cos^{2j-q} \omega \sin^q \omega \left[1 + \gamma \omega^2 \right]^{-m-h-j} d\omega, \end{aligned}$$

and where $\gamma = \rho^2 / [4\pi^2 (\lambda^2 - r^2)]$. Moreover, noting that when q is an odd number, the integral is equal to zero; therefore, q can be replaced with $2q$:

$$\begin{aligned} W_m &= \sum_{q=0}^{\lfloor j \rfloor} \binom{2j}{2q} \cos^{2(j-q)} \varphi \sin^{2q} \varphi \int_{-\pi}^{\pi} \cos^{2(j-q)} \omega \sin^{2q} \omega \left[1 + \gamma \omega^2 \right]^{-m-h-j} d\omega \\ &= \sum_{q=0}^{\lfloor j \rfloor} \sum_{p=0}^q \binom{2j}{2q} \binom{q}{p} (-1)^p \cos^{2(j-q)} \varphi \sin^{2q} \varphi \int_{-\pi}^{\pi} \cos^{2n} \omega \left[1 + \gamma \omega^2 \right]^{-m-h-j} d\omega, \end{aligned}$$

where $\lfloor l \rfloor$ signifies the largest integer that is not greater than l and $n = j - q + p$. Now, $\cos^{2n} \omega$ is expanded, as observed in ([30], Section 1.32); thus, W_m becomes

$$W_m = (1/2^{2n}) \sum_{q=0}^{\lfloor j \rfloor} \sum_{p=0}^q \binom{2j}{2q} \binom{q}{p} (-1)^p \cos^{2(j-q)} \varphi \sin^{2q} \varphi \left\{ \sum_{g=0}^{n-1} 2 \binom{2m}{g} W_{m_1} + \binom{2n}{n} W_{m_2} \right\},$$

where

$$\begin{aligned}
 W_{m_1} &= \int_{-\pi}^{\pi} \cos 2(n-g)\omega [1 + \gamma\omega^2]^{-m-k-j} d\omega \\
 &= \int_{-\pi}^{\pi} \sum_{s=0}^{\infty} (-1)^s \frac{2^{2s}(n-g)^{2s}}{(2s)!} \omega^{2s} [1 + \gamma\omega^2]^{-m-h-j} d\omega,
 \end{aligned}$$

By using substitution $V = \omega/\pi$ and then taking $D = V^2$, W_{m_1} thus becomes

$$\begin{aligned}
 W_{m_1} &= \pi \int_0^1 \sum_{s=0}^{\infty} (-1)^s \frac{2^{2s} \pi^{2s} (n-g)^{2s}}{(2s)!} D^{s-1/2} [1 + \gamma\pi^2 D]^{-n-h-i} dD \\
 &= 2\pi \sum_{s=0}^{\infty} (-1)^s \frac{2^{2s} \pi^{2s} (n-g)^{2s}}{(2s+1)(2s)!} F(m+h+j, s+1/2; s+3/2; -\pi^2\gamma).
 \end{aligned}$$

Additionally, W_{m_2} is given as

$$W_{m_2} = \int_{-\pi}^{\pi} [1 + \gamma\omega^2]^{-m-h-j} d\omega,$$

by taking $\Delta = \omega/\pi$, and then $Y = \Delta^2$. Thus, W_{m_2} becomes

$$W_{m_2} = \pi \int_0^1 Y^{-1/2} [1 + \pi^2\gamma Y]^{-m-h-j} dY = 2\pi F(m+h+j, 1/2; 3/2; -\pi^2\gamma).$$

Now, the interactions for the general case of helical angle $\psi = 12\pi/17$ is considered, where this value is the physical value of ψ , and it leads to the measured position of the minor and major grooves of the dsDNA. Thus, the total interaction, E_{tot_g} , in this case, may be obtained from

$$E_{tot_g} = \frac{a\rho\ell_{DG} \sin(\psi/2)}{2\pi} \int_{-\pi}^{\pi} \int_{-1}^1 E_p \sqrt{1 + \left(\frac{2a^2\pi \sin(\psi/2)}{\rho} \omega\right)^2} d\omega d\omega, \tag{4}$$

where $\ell_{DG} = 0.93 \text{ \AA}^{-2}$, and distance τ is given by

$$\begin{aligned}
 \tau^2 &= \left(\frac{a}{2} \left[\cos \omega + \cos(\omega - \psi) + \omega \left(\cos \omega - \cos(\omega - \psi) \right) \right] - \lambda \cos \varphi \right)^2 \\
 &+ \left(\frac{a}{2} \left[\sin \omega + \sin(\omega - \psi) + \omega \left(\sin \omega - \sin(\omega - \psi) \right) \right] - \lambda \sin \varphi \right)^2 + \left(\frac{\rho\omega}{2\pi} \right)^2.
 \end{aligned}$$

Noting that these integrals are extremely complicated, the integration packages in the Maple software are, therefore, used to obtain the numerical results.

3. Results and Discussion

In this section, the numerical solutions of Equations (3) and (4) are found by employing computer software Maple coupled with the aforementioned constants in the previous section titled ‘‘Mathematical modeling’’. By minimizing the interaction energies, the optimal rotational angle (φ) and distance (λ) from the z-axis of DNA are determined for the binding between the Cis and DNA molecules. We focus on the negative values for the total interaction energies, E_{tot_i} , between the Cis molecule and the dsDNA, where the negative values indicate that the binding process of Cis to dsDNA is energetically favorable. We start with the special case of $\psi = \pi$, where, in this case, the minor and major grooves are of equal size (17 Å). In Figure 3, the relation between the interaction energies E_{tot_s} and distance λ is plotted and $\varphi \in [0, 2\pi]$. Additionally, the interaction energies of the Cis and DNA molecules as a function of rotational angle φ are plotted for various values of distance

λ , as shown in Figure 4. The results observed that the minimum value of the interaction energies is approximately $E_{tot_S} \approx -17.5$ (kcal/mol), which is obtained for the values of $\lambda = 5.5 \text{ \AA}$ and $\varphi = \pi/2$ and $3\pi/2$ (i.e., when the center of Cis is perpendicular to the z-axis of the dsDNA). Furthermore, for the general case of the helical angle $\psi = 12\pi/17$, we note that the sizes of the minor and major grooves are 12 \AA and 22 \AA , respectively. Figures 5 and 6 show the relationship between the interactions, E_{tot_G} , the distance, λ , and the rotational angle φ for different values of the distance, λ , respectively. The results, in this case, indicate that the Cis molecule binds to both grooves in the DNA (minor and major), with the energy values being $E_{tot_G} \approx -6.4$ and $E_{tot_G} \approx -12.6$ (kcal/mol), respectively. As the interactions are dependent on the rotational angle, which lies within $(\pi, 2\pi)$ and $(0, \pi)$ for the minor and major grooves, respectively, the results show that the interaction of the Cis molecule with the major groove in the DNA is stronger than the minor groove, and this may result in a stable system after the interactions occur. In addition, the values of rotational angle φ and distance λ , which provide the minimum interaction energy, are ≈ 2.40 (rad) and $\approx 0.8 \text{ \AA}$ for the major groove and ≈ 5.40 (rad) and $\approx 12.60 \text{ \AA}$ for the minor groove, respectively. Moreover, a three-dimensional (3D) plot of the Cis molecule binding to the DNA is presented in Figure 7 for both cases, where the “LimeGreen” color in Figure 7b is for the major groove, and the “Navy” color is for the minor groove. The results are in excellent agreement with those provided in [11–16,18,19], where the main results of these studies showed that the Cis molecule targets the major groove in the DNA. This study can provide more explanations for the interactions between the Cis molecule and DNA; moreover, it may assist in the reduction in side effects of the Cis drug on DNA functions, and there are also some details about the binding of the Cis molecule to the DNA. Moreover, the present mathematical models studied the interactions in the binding of the Cis anticancer drug to DNA, which may help to understand these interactions and can assist in enabling a stronger drug at similar dosages, and that has fewer side effects, improving the chemical stability and biocompatibility. The mathematical models can also offer overall guidelines for future related research studies on molecular dynamics simulations and experiments. We note that the L–J potential is typically used for determining nonpolar interactions; this model only provides a first approximation in the system because the Cis molecule might also generate other interactions with the DNA. Notably, in this analysis study, not all interactions were taken into account; therefore, we may have different results in some cases, and this may also be because of the physical parameters and the geometric structure that have been adopted. Further research studies should examine the interactions between different drug molecules, such as carboplatin and doxorubicin, with dsDNA, ssDNA, and RNA.

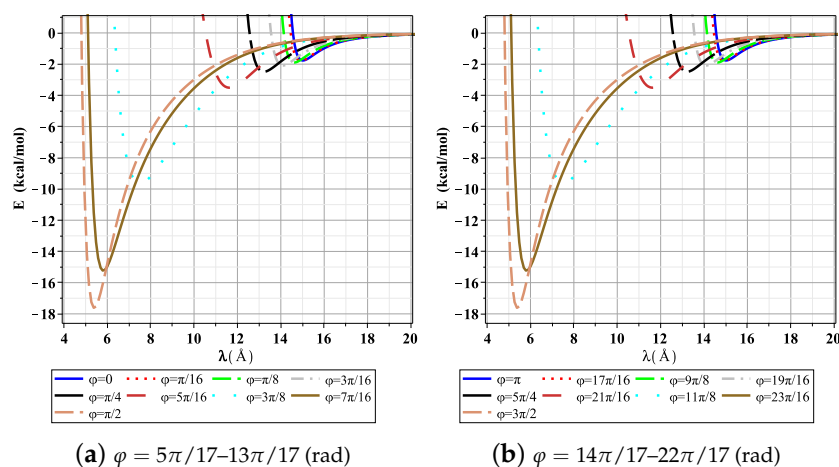


Figure 3. Cont.

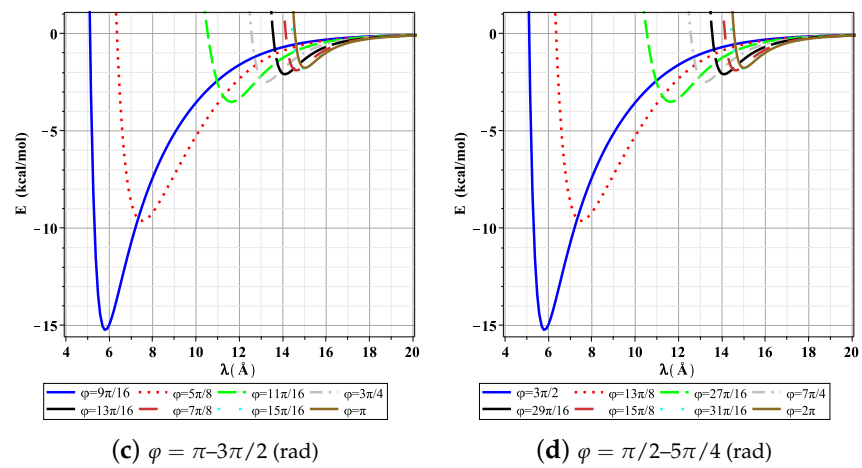


Figure 3. Energies of Cis molecules binding to DNA with respect to λ for $\psi = \pi$.

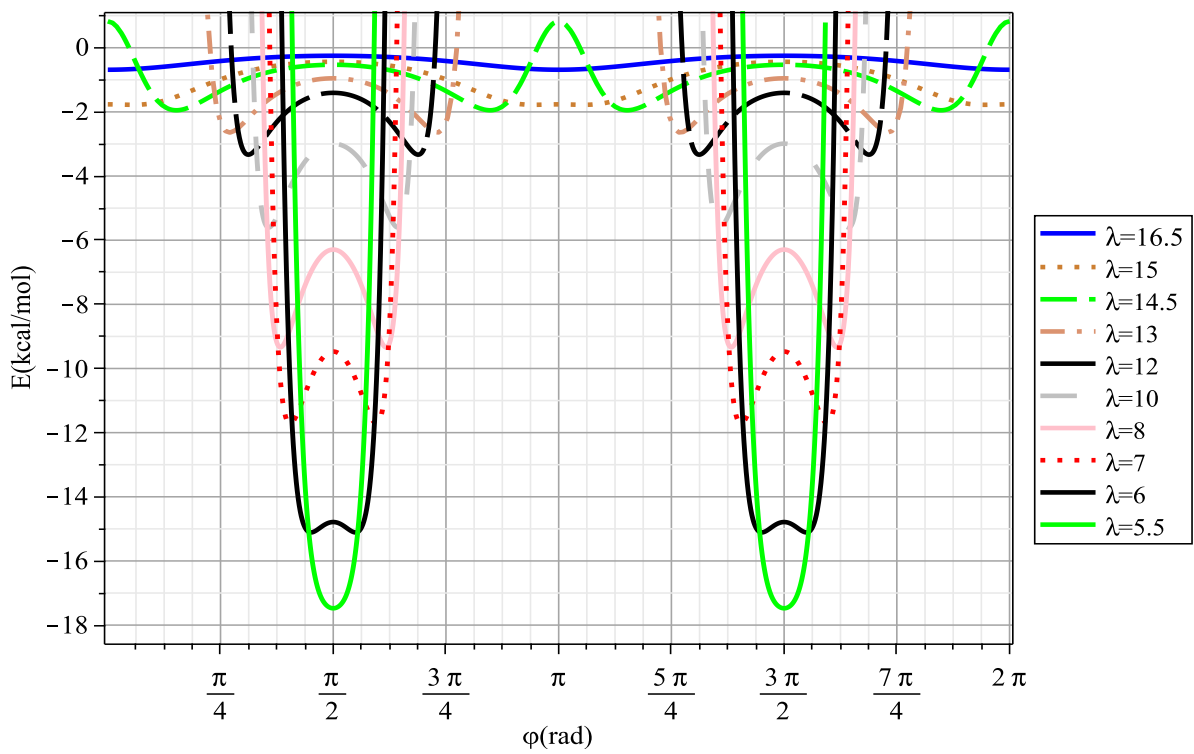


Figure 4. Total energies of Cis molecules binding to DNA with respect to ϕ for $\psi = \pi$.

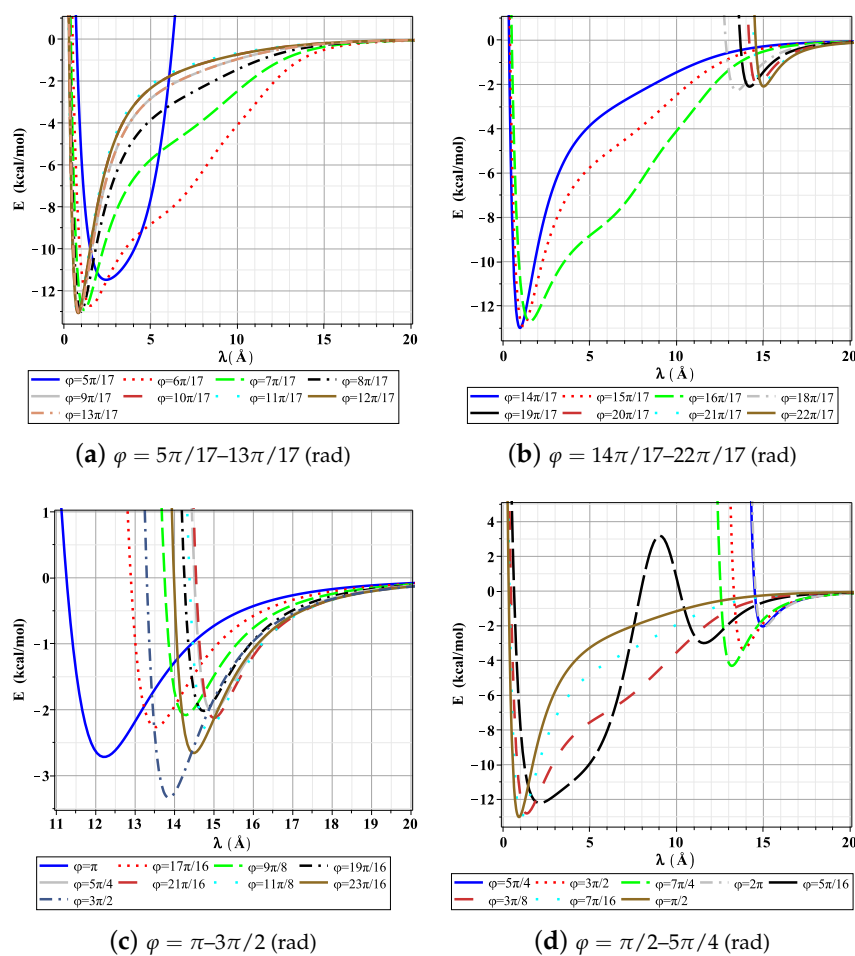


Figure 5. Energies of Cis binding to DNA with respect to λ for $\psi = 12\pi/17$.

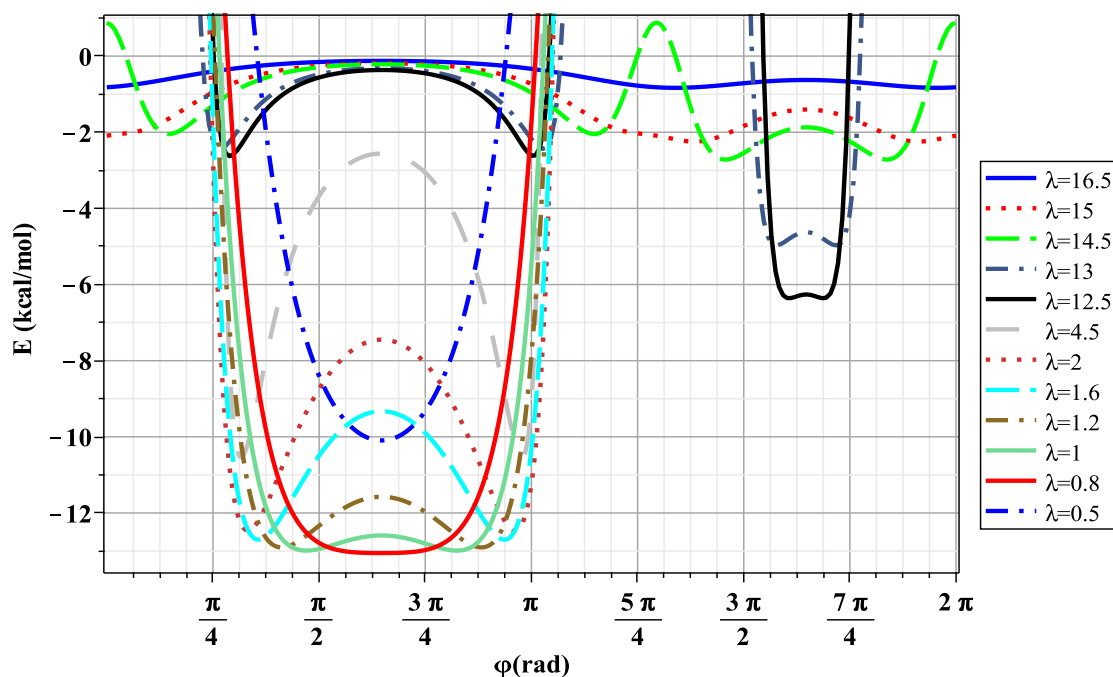


Figure 6. Energies of Cis molecules binding to dsDNA with respect to φ for $\psi = 12\pi/17$.

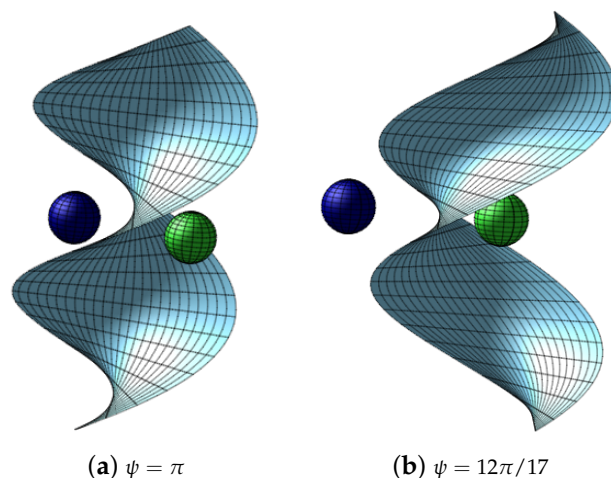


Figure 7. Three-dimensional plot of Cis molecules binding to dsDNA.

4. Summary

In this study, the interactions between the Cis and DNA molecules were determined using a classical modeling approach, and then the results were used to describe the mechanism by which cisplatin binds to dsDNA. The analytical expressions are provided for the special case of the dsDNA, and then the numerical solutions were found by using Maple software for both cases of the dsDNA. By minimizing the interaction energies for arbitrary distances, λ , and arbitrary tilt angles, φ , from the center of the Cis molecule to the z-axis of the dsDNA, the results observed that the Cis molecule binds to the dsDNA with a binding energy of -17.5 (kcal/mol) for the special case. In addition, the results of the general case of dsDNA suggested that the cisplatin molecule prefers to bind to the major groove in the dsDNA with a binding energy of -12.6 (kcal/mol), a distance of $\lambda = 0.8$ Å, and a tilt angle of $\varphi = 2.4$ rad. The fundamental and ideal behavioral model of cisplatin binding to DNA was formulated in this study, and the results can provide novel insights for understanding the molecular mechanism of the binding of the drugs to DNA. Nonetheless, more work is still required, especially for the interaction and mobility of DNA with different molecules, such as water, which is provided in physical systems.

Funding: This project was supported by Researchers Supporting Project number (RSP2023R411), King Saud University, Riyadh, Saudi Arabia.

Data Availability Statement: Not applicable.

Conflicts of Interest: The author declares no conflict of interest.

References

1. Drexler, K.E. *Nanosystems: Molecular Machinery, Manufacturing, and Computation*; John Wiley & Sons Inc.: Hoboken, NJ, USA, 1992.
2. Cui, D. Biomolecules functionalized carbon nanotubes and their applications. In *Medicinal Chemistry and Pharmacological Potential of Fullerenes and Carbon Nanotubes*; Carbon Materials: Chemistry and Physics; Springer: Dordrecht, The Netherlands, 2008; Volume 1, pp. 181–221.
3. Xu, X.; Li, R.; Ma, M.; Wang, X.; Wang, Y.; Zou, H. Multidrug Resistance Protein P-Glycoprotein Does Not Recognize Nanoparticle C₆₀: Experiment and Modeling. *Soft Matt.* **2012**, *8*, 2915–2923. [[CrossRef](#)]
4. Kamiya, K.; Okada, S. Energetics and Electronic Structure of Encapsulated Single-Stranded DNA in Carbon Nanotubes *Phys. Rev. B* **2011**, *83*, 155444. [[CrossRef](#)]
5. Watson, J.D.; Crick, F.H.C. Molecular Structure of Nucleic Acids: A Structure for Deoxyribose Nucleic Acid. *Nature* **1953**, *171*, 737–738. [[CrossRef](#)]
6. Alberts, B.; Johnson, A.; Lewis, J.; Raff, M.; Roberts, K.; Walter, P. *Molecular Biology of the Cell*; Garland Science: New York, NY, USA, 2008.
7. Duderstadt, K.E.; Chuang, K.; Berger, J.M. DNA stretching by bacterial initiators promotes replication origin melting. *Nature* **2011**, *478*, 209–213. [[CrossRef](#)] [[PubMed](#)]

8. Dasari, S.; Tchounwou, P.B. Cisplatin in cancer therapy: Molecular mechanisms of action. *Eur. J. Pharmacol.* **2014**, *5*, 364–378. [[CrossRef](#)]
9. Jamieson, E.R.; Lippard, S.J. Structure, recognition, and processing of cisplatin-DNA adducts. *Chem. Rev.* **1999**, *99*, 2467–2498. [[CrossRef](#)]
10. Dutta, S.; Rivetti, C.; Gassman, N.R.; Young, C.G.; Jones, B.T.; Scarpinato, K.; Guthold, M. Analysis of single, cisplatin-induced DNA bends by atomic force microscopy and simulations. *J. Mol. Recognit.* **2018**, *31*, e2731. [[CrossRef](#)]
11. Wing, R.M.; Pjura, P.; Drew, H.R.; Dickerson, R.E. The primary mode of binding of cisplatin to a B-DNA dodecamer: C-G-C-G-A-A-T-T-C-G-C-G. *EMBO J.* **1984**, *3*, 1201–1206. [[CrossRef](#)]
12. Takahara, P.; Rosenzweig, A.; Frederick, C.; Lippard, S.J. Crystal structure of double-stranded DNA containing the major adduct of the anticancer drug cisplatin. *Nature* **1995**, *377*, 649–652. [[CrossRef](#)]
13. Takahara, P.M.; Frederick, C.A.; Lippard, S.J. Crystal Structure of the Anticancer Drug Cisplatin Bound to Duplex DNA. *J. Am. Chem. Soc.* **1996**, *118*, 12309–12321. [[CrossRef](#)]
14. van Boom, S.S.G.E.; Yang, D.; Reedijk, J.; van der Marel, G.A.; Wang, A.H.-J. Structural Effect of Intra-strand Cisplatin-crosslink on Palindromic DNA Sequences. *J. Biomol. Struct. Dyn.* **1996**, *13*, 989–998. [[CrossRef](#)] [[PubMed](#)]
15. Gasior-Glogowska, M.; Malek, K.; Zajac, G.; Baranska, M. A new insight into the interaction of cisplatin with DNA: ROA spectroscopic studies on the therapeutic effect of the drug. *Analyst* **2016**, *141*, 291–296. [[CrossRef](#)] [[PubMed](#)]
16. Sip, M.; Schwartz, A.; Vovelle, F.; Ptak, M.; Leng, M. Distortions Induced in DNA by cis-Platinum Interstrand Adducts. *Biochemistry* **1992**, *31*, 2508–2513. [[CrossRef](#)] [[PubMed](#)]
17. Gelasco, A.; Lippard, S.J. NMR Solution Structure of a DNA Dodecamer Duplex Containing a cis-Diammineplatinum(II) d(GpG) Intrastrand Cross-Link, the Major Adduct of the Anticancer Drug Cisplatin. *Biochemistry* **1998**, *37*, 9230. [[CrossRef](#)]
18. Bellon, S.F.; Lippard, S.J. Bending studies of DNA site-specifically modified by cisplatin, trans-diamminedichloroplatinum(II) and cis-[Pt(NH₃)₂(N³-cytosine)Cl]⁺. *Biophys. Chem.* **1990**, *35*, 179–188. [[CrossRef](#)]
19. Bellon, S.F.; Coleman, J.H.; Lippard, S.J. DNA Unwinding Produced by Site-Specific Intrastrand Cross-Links of the Antitumor Drug cis-Diamminedichloroplatinum(II). *Biochemistry* **1991**, *30*, 8026–8035. [[CrossRef](#)]
20. Crisafuli, F.A.P.; Cesconetto, E.C.; Ramos, E.B.; Rocha, M.S. DNA—Cisplatin interaction studied with single molecule stretching experiments. *Integr. Biol.* **2012**, *4*, 568–574. [[CrossRef](#)]
21. Huang, H.; Zhu, L.M.; Reid, B.R.; Drobný, G.P.; Hopkins, P.B. Solution structure of a cisplatin-induced DNA interstrand cross-link. *Science* **1995**, *270*, 1842–1845. [[CrossRef](#)]
22. Baowan, D.; Cox, B.J.; Hilder, T.A.; Hill, J.M.; Thamwattana, N. *Modelling and Mechanics of Carbon-Based Nanostructured Materials*, 1st ed.; William Andrew: Norwich, NY, USA, 2017.
23. Jan, R.; Shah, Z.; Deebani, W.; Alzahrani, E. Analysis and dynamical behavior of a novel dengue model via fractional calculus. *Int. J. Biomath.* **2022**, *15*, 2250036. [[CrossRef](#)]
24. Alshehri, M.H. Continuum Modelling for Encapsulation of Anticancer Drugs inside Nanotubes. *Mathematics* **2021**, *9*, 2469. [[CrossRef](#)]
25. Pico, J.; Tang, T.-Q.; Shah, Z.; Bonyah, E.; Jan, R.; Shutaywi, M. Alreshidi, N. Modeling and Analysis of Breast Cancer with Adverse Reactions of Chemotherapy Treatment through Fractional Derivative. *Comput. Math. Methods Med.* **2022**, *2022*, 5636844.
26. Shah, Z.; Jan, R.; Kumam, P.; Deebani, W.; Shutaywi, M. Fractional Dynamics of HIV with Source Term for the Supply of New CD4+ T-Cells Depending on the Viral Load via Caputo-Fabrizio Derivative. *Molecules* **2021**, *26*, 1806. [[CrossRef](#)]
27. Ferrari, M. Cancer nanotechnology: Opportunities and challenges. *Nat. Rev. Cancer* **2005**, *5*, 161–171. [[CrossRef](#)]
28. Maitland, G.C.; Rigby, M.; Smith, E.B.; Wakeham, W.A. *Intermolecular Forces—Their Origin and Determination*; Clarendon Press: Oxford, UK, 1981.
29. Rappi, A.K.; Casewit, C.J.; Colwell, K.S.; I, W.A.G.I.I.; Skid, W.M. UFF, a full periodic table force field formolecular mechanics and molecular dynamics simulations. *J. Am. Chem. Soc.* **1992**, *114*, 10024–10035. [[CrossRef](#)]
30. Gradshteyn, I.S.; Ryzhik, I.M. *Table of Integrals, Series, and Products*, 7th ed.; Academic Press: New York, NY, USA, 2007.
31. Cox, B.J.; Thamwattana, N.; Hill, J.M. Mechanics of atoms and fullerenes in single-walled carbon nanotubes. I. Acceptance and suction energies. *Proc. R. Soc. A Math. Phys. Eng. Sci.* **2007**, *463*, 461–477. [[CrossRef](#)]
32. Erdelyi, A.; Magnus, W.; Oberhettinger, F.; Tricomi, F.G. *Higher Transcendental Functions Vol I*; McGraw-Hill: New York, NY, USA, 1953.

Disclaimer/Publisher’s Note: The statements, opinions and data contained in all publications are solely those of the individual author(s) and contributor(s) and not of MDPI and/or the editor(s). MDPI and/or the editor(s) disclaim responsibility for any injury to people or property resulting from any ideas, methods, instructions or products referred to in the content.